14TH CANADIAN MASONRY SYMPOSIUM
MONTREAL, CANADA
MAY 16TH – MAY 20TH, 2021

REVIEW OF PERFORMANCE ASSESSMENT REQUIREMENTS FOR URM WALLS

Anghaie, Hamid[1] and Pantazopoulou, S.J. (Voula)[2]

ABSTRACT

Historic and heritage buildings form a significant part of the built environment in many urban areas across Canada. Having a lifetime of more than a hundred years, many of them comprise load-bearing unreinforced masonry (URM) walls. The Canadian earthquake engineering community has been gearing towards adaptation of a consequence–based seismic assessment framework for masonry structures. In this case, determining pertinent acceptance criteria (i.e. dependable estimations of deformation capacity) that ought to be linked to the reference performance objectives (degree of negotiable damage) are of primary interest to structural engineers. This paper provides a general review of the current seismic provision guidelines in ASCE/SEI41-17 and the draft version of the new Eurocode 8-III Chapter 11 (2022). The objective is to build up the background of technical guidelines for the seismic assessment of URM walls that would lay the ground for establishing seismic assessment and retrofit procedures for URM structures across Canada for the future editions of the Canadian seismic codes.

KEYWORDS: *acceptance criteria, seismic assessment, seismic provision guidelines, unreinforced masonry*

[1] PhD Candidate, Department of Civil Engineering, The Lassonde Faculty of Engineering, York University, 4700 Keele St, Toronto, ON, Canada, hamidang@yorku.ca

[2] Professor, Department of Civil Engineering, The Lassonde Faculty of Engineering, York University, 4700 Keele St, Toronto, ON, Canada, pantazo@yorku.ca

INTRODUCTION

Unreinforced Masonry Walls and Earthquakes

Reports from past earthquakes show that many older unreinforced masonry (URM) buildings have suffered extensive damage, and yet many others have experienced little damage over centuries after enduring multiple earthquake events [1]. In the context of assessment it is critical to be able to identify those structures that are most vulnerable to damage, and for this reason it is important to understand the parameters that trigger catastrophic failure in this class of structures. Falling material due to global in-plane shear damage or local out-of-plane instability is the most common type of seismic damage in URM walls [2], whereas in general, out-of-plane failure often initiates earlier than in-plane failure mechanisms [2]. Satisfactory seismic performance of a structure is only achieved if the performance objectives regarding its global behavior can precede the occurrence of local failure mechanisms such as out-of-plane wall failure [3].

IN-PLANE SEISMIC PERFORMANCE OF URM WALLS

In-plane Failure Mechanisms of URM Walls

The 2017 edition of ASCE/SEI41 specifies 5 primary in-plane response mechanisms for URM walls. These are, flexural (rocking), bed-joint shear sliding (leading either to single bed-joint cracking or to stair-step cracking through head and bed joints), toe crushing, diagonal tension (that causes cracking through the masonry units), and vertical compression. The first two failure modes are categorized in ASCE/SEI41 as deformation-controlled actions and the next three modes are considered force-controlled actions. Deformation-controlled mechanisms represent a ductile behavior in which the displacement capacity extends beyond the notional yield point (this is the point in the idealized bilinear force-displacement response where a sharp change of stiffness occurs). Force-controlled mechanisms represent a non-ductile behavior in which the demand cannot exceed the nominal strength of the component. Flexural rocking mode and bed-joint shear sliding modes are more probable in URM piers with low level of vertical axial stress [2].

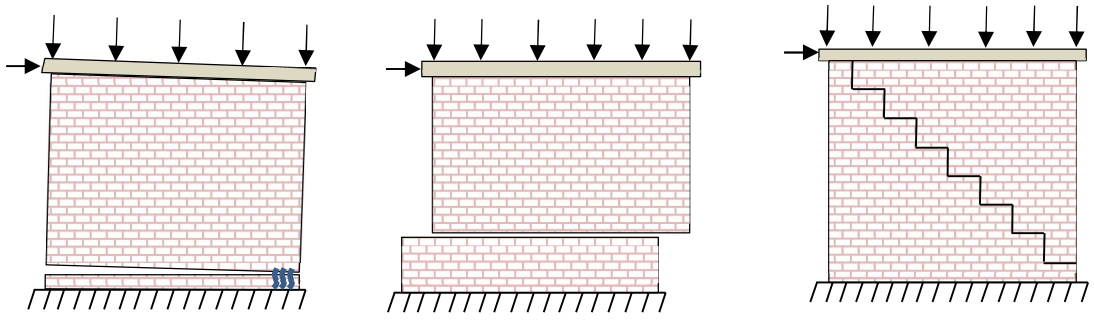

a) Flexural Failure **b) Bed-joint Shear Sliding** **c) Diagonal Cracking**

Figure 1: In-plane Failure Mechanisms of URM Walls/Piers

The higher the level of the vertical axial stress is, the more probable it will be that the URM pier would exhibit a diagonal tension failure mode or toe-crushing failure mode [2], [4]. Toe crushing

can be regarded as a secondary yield mechanism at large drift levels (after rocking initiates) for URM wall piers that are subjected to high axial loads [2]. Key factors that affect the in-plane seismic behavior of an URM wall are the aspect ratio, the vertical overburden pressure, the boundary conditions (shear span), the size effect, the previous loading history (monotonic or cyclic), and the mechanical properties (thickness of mortar joints, strength of masonry blocks and mortar, material stiffnesses, cohesion at the mortar-brick interface) of the masonry. Hybrid failure modes are also common in URM wall pier experiments [2]. In ASCE/SEI41-17, a URM wall or pier is specified as a deformation-controlled component if Equation 1 is satisfied [2]:

$$Min\{V_r, V_s\} \le Min\{V_c, V_d\} \tag{1}$$

Here, V_r is the expected rocking strength of the URM wall or pier, V_s is the expected bed-joint sliding strength, V_c is the lower-bound toe-crushing strength, and V_d is the lower-bound diagonal tension strength of the URM wall or pier, which are obtained from Equations 2 to 5, respectively:

$$V_r = 0.45(N+W)\cdot\left(\frac{L}{h_{eff}}\right) \tag{2}$$

$$V_s = f_v \cdot A_n \tag{3}$$

$$V_c = 0.5(N+W)\cdot\left(\frac{L}{h_{eff}}\right)\cdot\left(1-\frac{\sigma_0}{0.7 f_m}\right) \tag{4}$$

$$V_d = f_t \cdot A_n \cdot \beta \cdot \sqrt{1+\frac{\sigma_o}{f_t}} \tag{5}$$

N is the overbearing axial load, W is the wall self-weight, L is the length of the wall cross section, h_{eff} is the height of the wall from the critical section at the base, to the resultant of seismic force, f_v is the bed-joint sliding shear strength (which comprises a cohesion and a frictional contribution according with the expression: $f_v = 0.5 \,.\, (\eta \,.\, f_{v0} + ((N + W)/A_n))$, $\eta = 1.0$ or 0.75 for single or double wythe walls, A_n is the area of net mortared or grouted section of the wall, σ_0 is the axial compression stress caused by gravity loads, f_m is the masonry compressive strength, f_t is the masonry diagonal tension strength, and β ranges between 0.67 and 1 depending on the L/h_{eff} ratio. Note that V_c limits V_r (i.e., $V_r \le V_c$). If Eq. 1 is not satisfied, the URM wall or pier will be considered a force-controlled component. For deformation-controlled actions which are analyzed with a linear procedure, acceptance criteria are specified in terms of strength as is shown in Equation 6:

$$m \cdot \kappa \cdot Q_{CE} \ge Q_{UD} \tag{6}$$

Here, Q_{UD} are the estimated demands for the earthquake load combination ($E+G$), Q_{CE} is the expected strength of the component, the m-factor is applied to account for the ductility demand

($1 \leq m \leq 3$). A knowledge factor κ is applied to account for any uncertainty associated with component as-built information ($0.75 \leq \kappa \leq 1.0$). For deformation-controlled actions which are analyzed with a nonlinear procedure, the acceptance criteria are specified in terms of deformation demands (δ_{req}) which are compared with the deformation capacities (δ_u) as shown in Eq. 7:

$$\kappa \cdot \delta_u \geq \delta_{req} \tag{7}$$

Acceptance criteria for force-controlled actions are specified in terms of lateral load resistance in linear and nonlinear procedures.

Both assessment frameworks (ASCE/SEI-41 2017, and EC8-III 2022) distinguish between primary and secondary elements in the structure. Secondary elements are those that participate in resisting the vertical loads however their contribution to lateral stiffness is insignificant. The difference in lateral load resistance when neglecting in the model the members identified as secondary should not exceed 25% of the value obtained when considering them in the model. In this context secondary elements are checked against deformation criteria, which are generally more generous for this class of members as compared to the primary elements of the structure.

In-plane Drift Capacity of URM Walls

A performance-based methodology has been implemented in the modern seismic codes, including ASCE/SEI41 (2017) and Eurocode 8-III (2022), and hence, acceptance criteria for the elements that exhibit some ductility capacity are specified in terms of drift ratios for multiple performance levels. Drift ratio is the ratio of relative displacement of the two ends of a deformed member divided by the distance between them, while accounting for the rotation of the end supports. Three performance levels have been specified in ASCE/SEI41, referred to as Immediate Occupancy (IO), Life Safety (LS), and Collapse Prevention (CP) [2]. The corresponding damage limit states specified in ASCE/SEI41-17 for URM walls are summarized in Table 1. Similarly, in Eurocode8-III (2022), three performance levels have been specified, referred to as Damage Limitation (DL), Significant Damage (SD), and Near Collapse (NC) [5]. The NC limit state is commonly mapped to a 20% postpeak strength reduction, as is shown in Figure 2 (a). ASCE/SEI41 defines the IO limit state as the beginning of observable permanent damage (based on tests) and limits the deformation capacity at this state to be less than or equal to 0.67 times the deformation capacity at LS limit state, for both primary and secondary components, shown by letter P and S in Figure 2 (b). The deformation capacity for primary components at LS limit state is limited to ¾ of the deformation at point C in the figure, and for secondary components, it is limited to ¾ of the deformation at point E in the figure. For primary components at CP limit state, deformation is limited to that of point C in the figure but not greater than ¾ of the deformation at point E, and for secondary components, the deformation for the CP limit state is limited to that of point E [2].

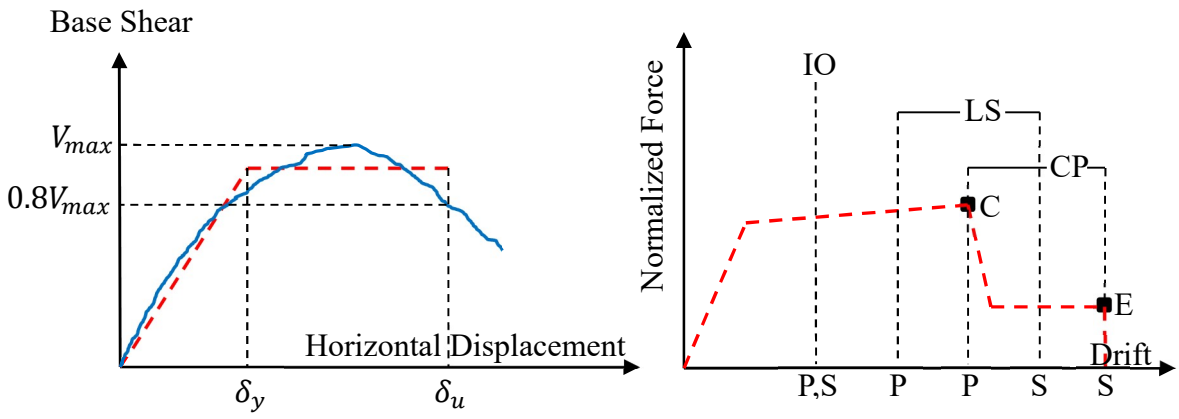

a) Idealized Bilinear Response **b) ASCE/SEI41, 2017**

Figure 2: In-plane Idealized Force-Displacement Response of a URM Wall/Pier

In the 2022 draft version of EC8-III (Chapter 11) the acceptance criteria for URM elements are specified at the DL, SD, and NC limit states. EC8-III (2022) defines the deformation capacities of URM piers while distinguishing between different failure modes, different masonry typologies (i.e. regular or irregular) and whether they are classified as modern or pre-modern masonry [5]. The values, given in terms of drift capacities as proposed for URM piers are summarized in Table 2 (subscripts $_f$, $_s$ and $_d$ correspond to the three resistance mechanisms described by Eqs. 2-5). Note that in Table 2, ν is the normalized axial load, obtained from Equation 8:

$$\nu = N_E / \left(L \cdot t \cdot f_m \right) \tag{8}$$

N_E is the design value of axial load at the critical section for the earthquake combination, t is the wall thickness, and f_m is the mean compressive strength of masonry as obtained from in-situ tests (or from additional sources of information) [5]. In EC8-III, the acceptance criteria at the NC limit state are defined as 4/3 of the drift ratio capacities at the SD limit state [5]. Figure 3(a) shows a generalized force-drift ratio relationship proposed in EC8-III for URM masonry elements, in which the ultimate drift ratio θ_u, corresponds to the onset of a reduction in lateral load resistance (the amount of reduction depends on the failure mechanism); a second ultimate drift ratio θ_{u2} is defined which corresponds to further reduction in the resistance, to a residual value. The intended use of these acceptance criteria is for concrete and brick masonry, but they are often applied to stone masonry as well due to the lack of alternative reference values [6].

Tables 3 and 4 present the modelling parameters and the drift ratio capacities proposed by ASCE/SEI41-17 for nonlinear analysis procedures for URM walls/piers with a lower-bound bed-joint shear strength test value, f_{v0}, equal or greater than 0.20 MPa (30 psi) (note that f_{v0} represents the cohesion, which is part of the f_v term in Eq. 3). ASCE/SEI41-17 classifies URM walls/piers as force-controlled if fv0 is less than 0.2MPa. Note that in Table 3, d, e, and f represent the

nonlinear deformation capacities as shown in Figure 3(b), c is the residual strength ratio of URM wall pier, V_c is the lateral load resistance associated with the onset of toe crushing after rocking initiates (defined prior to this), $\delta_{c,u}$ is the corresponding lateral displacement, h is the height of the wall, δ_y is the displacement at notional yielding, V_{s1} is the expected initial lateral resistance of wall or pier obtained from Equation 3, and V_{s2} is the expected residual lateral resistance of the wall obtained from Eq. 9 (N_d is the overbearing dead load):

$$V_{s2} = 0.5N_d \tag{9}$$

Russell and Ingham (2010) recommended a drift ratio limit of 0.4% for URM walls or piers that fail in a bed-joint shear sliding mode with a stair-step cracking pattern [2], [7]. Priestley et al., (2007) recommended a design drift ratio for a damage-control performance of 0.4-0.5% for URM walls that fail in shear, and suggested a design drift ratio of 0.8% for URM walls that are controlled by flexural rocking [1]. This was based on experimental evidence (Magenes & Calvi 1997) after subjecting brick masonry piers to cyclic in-plane quasi-static loads, and observing shear failures at ultimate drift ratios ranging between 0.44% - 0.62% [3], [8].

The drift ratio corresponding to the notional yield point at crack initiation (in the bilinear force-deformation response) in URM masonry walls θ_y, are in the range of 0.15%±0.05% for in-plane and 0.20% for out-of-plane wall deformation, associated with the IO limit state [10]. Vanin et al. (2017) reported that the drift ratio at the onset of cracking fell within 0.1 and 0.3% for most of the stone masonry walls based on a dataset of 123 quasi-static cyclic tests reported in the literature [6].

In the experimental investigations, the loading history, whether it is reversed cyclic or monotonic, significantly influences the drift capacities of URM wall piers. Based on experimental evidence, stone masonry wall specimens attained significantly larger drift capacities in monotonic, than in cyclic tests [6]. This has been also observed in the tests for clay block masonry walls [9].

Table 1: Structural Performance Levels for URM Walls (ASCE/SEI41, 2017)

Type	Structural Performance Levels		
	Immediate Occupancy	Life Safety	Collapse Prevention
Primary Elements	Minor cracking of veneers. Minor spalling in veneers at a few corner openings. No observable out-of-plane offsets.	Major cracking. Noticeable in-plane offsets of masonry. Minor out-of-plane offsets	Extensive cracking; face course and veneer might peel off. Noticeable in-plane and out-of-plane offsets
Secondary Elements	Same as for primary elements	Same as for primary elements	Non-bearing panels dislodge
Drift	Transient drift that causes minor or no non-structural damage. Negligible permanent drift.	Transient drift sufficient to cause non-structural damage. Noticeable permanent drift.	Transient drift sufficient to cause extensive non-structural damage. Extensive permanent drift.

Table 2: In-plane Drift Ratio Capacities of URM Walls/Piers (EC8-III, 2022)

Flexural (Rocking)			Bed-joint shear sliding			Diagonal shear cracking		
θ_{DL}	$\theta_{SD}=\theta_{f,u}$	$\theta_{NC}=\theta_{f,u2}$	θ_{DL}	$\theta_{SD}=\theta_{s,u}$	$\theta_{NC}=\theta_{s,u2}$	θ_{DL}	$\theta_{SD}=\theta_{d,u}$	$\theta_{NC}=\theta_{d,u2}$
elastic limit θ_y	(1- ν)%	$\left(\frac{4}{3}\right)\theta_{f,u}$	elastic limit θ_y	0.4%♣ or 0.5%♠ or 0.8%♦	$\left(\frac{4}{3}\right)\theta_{s,u}$	elastic limit θ_y	0.5%● or 0.6%▲	$\left(\frac{4}{3}\right)\theta_{d,u}$

♣For modern regular masonry, For pre-modern regular masonry: ♠block unit failure, or ♦sliding, ●For pre-modern irregular masonry, ▲For pre-modern regular masonry.

In EC8-III, an acceptance criterion for URM elements in the DL performance limit state is specified in terms of shear force as per Equation 10:

$$\gamma_{Sd} V \le V_R / \gamma_{Rd} \tag{10}$$

where, V is the shear demand associated with the DL performance limit state and it is increased by a partial factor γ_{Sd} to account for uncertainty in modelling the action effects $1.0 \le \gamma_{Sd} \le 1.15$, whereas V_R is the lateral load resistance, obtained from Equation 11:

$$V_R = min\{V_r, V_s, V_d\} \tag{11}$$

Here, V_r is the lateral load resistance associated with flexural failure, V_s is the shear resistance due to shear sliding, and V_d is the lateral load resistance associated with diagonal tension cracking. They are obtained from Equations 12 to 14 as follows:

$$V_r = \left(\frac{N}{2}\right)\cdot\left(1-1.15\nu\right)\cdot\frac{L}{h_{eff}} \tag{12}$$

$$V_s = d'\cdot t\cdot\left(f_{v0}+\frac{\mu\cdot N}{d'\cdot t}\right)\le V_{s,block} \tag{13}$$

$$V_d = \left(\frac{L.t}{b}\right)\cdot f_t\cdot\sqrt{1+\frac{\sigma_0}{f_t}}\ ; \tag{14}$$

Where, d' is the depth of the compression zone at the critical section of the pier, f_{v0} is the shear strength of masonry in the absence of axial load (owing to the cohesion of the mortar joint), μ is the masonry friction coefficient (taken equal to 0.5), b is a correction coefficient accounting for the shear stress distribution in the middle section of the panel and is related to the aspect ratio of

the panel ($1.0 \le b \le 1.5$), f_t is the diagonal tensile strength of masonry, and σ_0 is the mean vertical stress in the transverse section of the panel. In Eq. 13, $V_{s,block}$ is an upper limit to V_s associated with the diagonal compression failure of masonry units and may be obtained from Eq. 15 (f_b is the normalized compressive strength of the masonry units):

$$V_{s,block} = 0.065 f_b \cdot d' \cdot t \tag{15}$$

In Equation 10, the governing lateral load resistance, V_R is reduced by a partial factor γ_{Rd} to account for uncertainty in the material properties and its value is a function of the knowledge levels attained ($1.35 \le \gamma_{Rd} \le 2.15$).

In EC8-III (2022), the drift ratio capacity at the DL performance limit state is taken equal to θ_y, the yield drift ratio, which corresponds to the notional yield point in the idealized bilinear force-deformation relationship, where the masonry is assumed to be in an elastic cracked condition (see Fig. 2(a)). For the SD and NC performance limit states, the acceptance criteria in EC8-III are specified in terms of drift ratio as shown in Eq. 16 for the SD and NC limit states, respectively:

$$\gamma_{Sd}\rho_{SD}\theta \le \theta_{SD} / \gamma_{Rd} \quad ; \quad \gamma_{Sd}\rho_{NC}\theta \le \theta_{NC} / \gamma_{Rd} \tag{16}$$

Factors ρ_{SD} and ρ_{NC} are used to amplify the deformation demand, θ, at the SD and NC limit states, respectively (for more details, refer to [5]), and γ_{Rd} is a partial factor accounting for the uncertainty in the resistance (in terms of deformation) which depends on the knowledge levels attained ($1.7 \le \gamma_{Rd} \le 1.85$).

As an illustrative example of the predictions obtained from the two code frameworks, the shear span of a doubly clamped unreinforced brick masonry wall with a regular running bond pattern is considered. The URM wall has a length L of 2m, an effective height, h_{eff} (distance from peak flexural moment to point of inflection) of 1.5m, a thickness t of 0.2m and it is subjected to a uniform overbearing pressure equal to $\sigma_0 = 0.5$MPa. The weight per unit volume of the masonry is assumed to be 1800 kg/m^3 for this example. The net mortared section of the wall is assumed to be equal to the gross section of the wall. The additional properties assumed in order to estimate the shear resistance of the wall according to ASCE/SEI-41 (2017) and EC8-III (2022) is presented in Table 5, where all the variables have been defined in the previous sections.

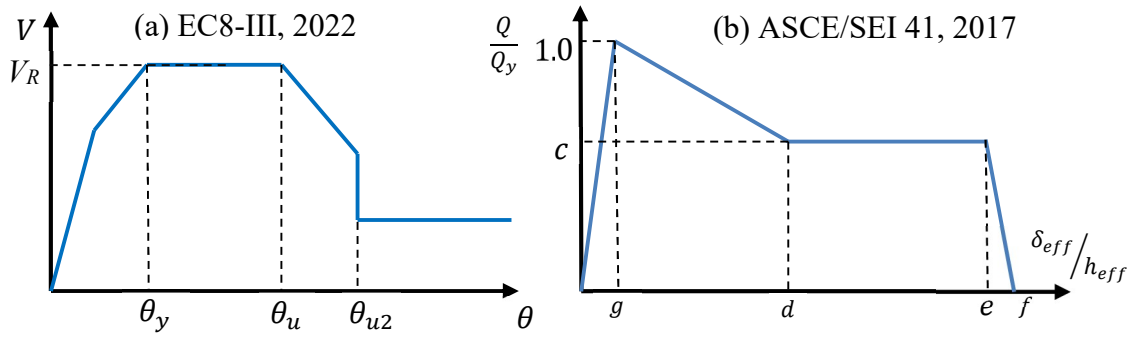

Figure 3: Generalized Force-Drift ratio Relationship for URM Elements

Table 3: Modelling Parameters for URM Walls with $f_{v0} \geq 0.2$ *MPa* (ASCE/SEI41, 2017)

Limiting Behavior Mode for URM Walls/Piers	Modelling Parameters			
	c	*d*	*e*	*f*
Rocking	V_c / V_r	$\delta_{c,u} / h_{eff}$ %	$\delta_{c,u} / h_{eff}$ %	$\frac{\delta_{c,u} + \delta_y}{h_{eff}}$ %
Bed-joint sliding	V_{s2} / V_{s1}	0.4%	1.0%	$1.0 + \frac{\delta_y}{h}$ %

Table 4: Drift ratio Capacities for URM Walls with $f_{v0} \geq 0.2$ *MPa* (ASCE/SEI41, 2017)

Limiting Behavior Mode		Drift Ratio limits		
		IO	LS	CP
Rocking	Simplified	0.1%	$0.4h_{eff}/L \leq 1.5\%$	$0.6h_{eff}/L \leq 2.25\%$
	Comprehensive	0.1%	$0.6h_{eff}/L \leq 2.25\%$	$\delta_{c,u}/h_{eff} \leq 2.5\%$
Bed-joint Sliding		0.1%	0.75%	1.0%

Table 5: Material Properties of Wall Example

f_m (MPa)	f_{v0} (MPa)	f_t (MPa)	f_b (MPa)	σ_0 (MPa)	μ
4.0	0.3	0.5	20.0	0.5	0.5

Table 6 lists the values of strength and deformation corresponding to the reference limit states calculated according to the two assessment frameworks described in the preceding. The depth of the effective compression zone d' is estimated as 0.29m. The following values have been used for the input parameters: $\beta=1$, $N=200$ *kN*, $W=10.6$ *kN*, $b=1$. The overbearing axial load, *N*, is obtained by multiplying the overbearing pressure by the gross area of the wall. According to ASCE/SEI41 this wall would be considered as a force-controlled component as Equation 1 is not satisfied and

the toe crushing strength governs the failure mode of the wall. It is noted that the ASCE/SEI41 expression overestimates the sliding resistance of the wall pier because it accounts for the entire grouted wall surface without consideration of uplift in the tension zone. In contrast, the EC8-III only accounts for the part of the cross section that is under normal compression, leading to more conservative estimate for this term, which eventually governs the wall resistance.

Table 6: Calculated Wall Resistance and Deformation Limit States

Lateral Resistance Estimate	ASCE/SEI41-17	EC8-III (2022)
V_r (kN)	126	114
V_s (kN)	160	100
V_c (kN)	115	-
V_d (kN)	283	283
V_R (Governing) (kN)	115	100
Drift ratio capacity	At IO state: = 0.1%	At DL state: ≤ 0.15%
Drift ratio capacity	At LS state: = 0.3%	At SD state: ≤ 0.8%
Drift ratio capacity	At CP state: = 0.45%	At NC state: ≤ 1.06%

OUT-OF-PLANE SEISMIC PERFORMANCE OF URM WALLS

After the initiation of in-plane failure mechanisms in an URM wall, if there is no out-of-plane movement, provided that the URM wall still supports the gravity load in its plane, collapse is considered to have been mitigated. But, out-of-plane deformation on its own can lead to the collapse of the wall [11]. Note that out of plane action occurs due to the inertia forces of the walls that are oriented normal to the seismic action. For example, considering the wall example discussed in the preceding (1800 kg/m^3), for a response acceleration corresponding to the fundamental period of the building in the range of 0.3g, it follows that a distributed inertial pressure in the order of 1 MPa pushes the wall outwards. Both strength and instability are controlled by the magnitude of the axial load and the eccentricity of its line of action from the pivot of rotation of the wall as it rocks out-of-plane. Based on experimental evidence, the acceptance criteria for the out-of-plane response of an URM wall are specified in terms of displacement [1].

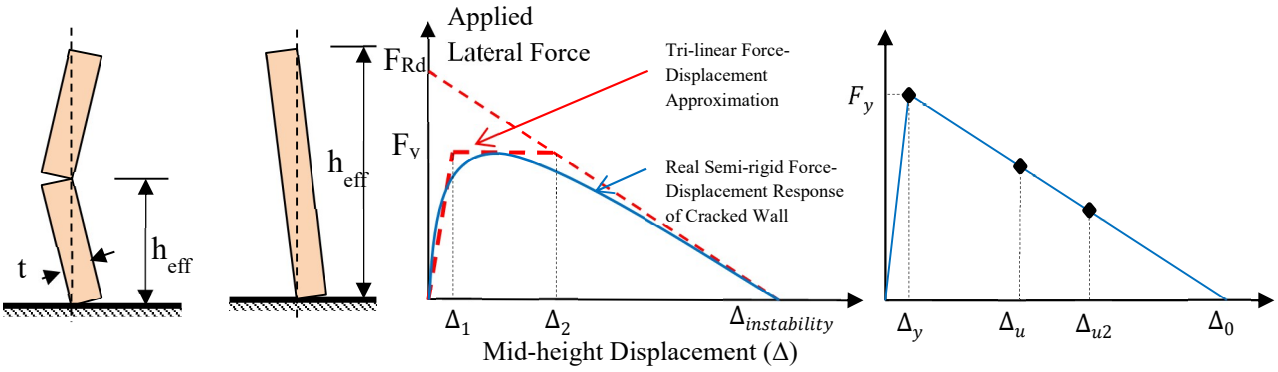

a) Out of Plane Rocking b) Adapted from [12] c) Adapted from EC8-III, (2022)

Figure 4: Out-of-plane Force-Displacement Response of URM Walls/Piers

The out-of-plane response of a URM wall is significantly affected by the boundary conditions. In a case of double clamped wall subjected to out-of-plane loading, the wall behaves like a vertical beam in bending acted upon by the lateral inertia pressures estimated above, and by the overbearing axial load; it has been experimentally observed that the wall will crack just above the mid-height, which results in the rocking of both top and bottom wall segments in the out-of-plane direction [11], as depicted in Fig. 4(a). In this case, the location of the crack should be considered in the analytical modeling of URM walls to better capture their out-of-plane response. In a case where the URM wall is loosely fixed at the top and rotating at the base, the wall behaves like a cantilever and shows much less resistance to overturn [2]. It is noteworthy that the in-plane behavior of URM wall piers is often governed by material nonlinearity while the out-of-plane behavior is governed by geometrical nonlinearity (P-Delta effects) as can be seen in Fig 4 (b). According to ASCE/SEI41-17, for in-plane drift ratios greater than 1.5%, the response might deteriorate due to out-of-plane effects (e.g., rotating of piers about their toe) [2].

The acceptance criteria for the out-of-plane response of URM walls in ASCE/SEI41-17 are specified for the three performance levels mentioned in the preceding. For the IO Level, ASCE/SEI does not permit flexural cracking resulting from out-of-plane inertial loading. For the LS level, ASCE/SEI considers a cracked wall to have out-of-plane stability during a seismic event if the height to thickness ratio of the wall is less than or equal to 8 (for more details, refer to [2]). For the CP level, ASCE/SEI suggests that the height to thickness ratio of the wall be limited and a value of 8 is set as a reasonable lower limit [2]. EC8-III considers three limit states for the out-of-plane response of URM wall piers, which are shown in Figure 4(c) by Δ_y, Δ_u, and Δ_{u2}. Yield displacement Δ_y corresponds to the DL limit state which is the onset of loss of contact at the pivot (onset of rocking), Δ_u corresponds to the SD limit state which corresponds to the rocking behavior but still far from collapse, and Δ_{u2} corresponds to the NC limit state. The toppling strength F_{Rd} (the intercept of the idealized bilinear out-of-plane response with the vertical axis) is calculated from Equation 17 as follows:

$$F_{Rd} = \lambda \cdot W \cdot (1 + \Psi) \cdot \frac{t}{h_{eff}} \quad ; \quad \Psi = 2N_E / W \tag{17}$$

Coefficient λ is equal to 1 or 2 depending on whether the wall is cantilever or clamped at top and bottom, respectively (see Fig. 4(a)), and N_E is the axial load carried by the wall in the earthquake combination. In Fig. 4(c) F_y is the notional yielding resistance of the wall in the out of plane action (i.e., the total lateral force that would cause at the critical section of the wall the development of its flexural strength). Note that for a URM wall the flexural strength is provided by the limited tensile strength of the masonry or to the action of the overbearing axial load (following a similar expression as in Eq. 12, where L is replaced by the wall thickness, t).

CONCLUSIONS

Modern seismic assessment codes ASCE/SEI41 (2017), and Eurocode 8-III (2022) have implemented performance-based provisions for the seismic evaluation of existing URM walls, limiting the drifts of the structure at multiple performance limit states. A vast number of experimental studies have been going on in the last decade to better understand the seismic performance of URM walls and to provide a framework for a displacement-based assessment of masonry structures. Based on the literature reviewed in this study, the drift thresholds at the onset of the specified performance limit states for URM wall piers are a function of their failure mode and they all fall within the range of 0.1% to 1.0%. The example illustrated that the deformation capacities for rocking/toe crushing can be significantly smaller than that associated with sliding whereas the corresponding strength terms are rather close (within the uncertainty levels embedded in the calculation of the two terms).

REFERENCES

[1] Priestley, M. J. N., Calvi, G. M., and Kowalsky, M. J., 2007, "Displacement-Based Seismic Design of Structures", Fondazione EUCENTRE, Pavia, Italy.

[2] American Society of Civil Engineers (ASCE), 2017, "Seismic Evaluation and Retrofit of Existing Buildings", ASCE/SEI Standard 41-17, Reston, VA, USA.

[3] Allen, C., Masia, M., Derakhshan, H., Griffith, M., Dizhur, D., Ingham, J., 2013, "What Ductility Value Should be Used When Assessing Unreinforced Masonry Buildings?", New Zealand Society of Earthquake Engrg Conference, April 2013, Wellington, New Zealand.

[4] Moon, F. L., 2004, "Seismic strengthening of low-rise unreinforced masonry structures with flexible diaphragms" Ph.D thesis, Georgia Institute of Technology, Atlanta.

[5] Eurocode 8: Design of structures for earthquake resistance, Part 3: Assessment and retrofitting of buildings. Technical Report EN 1998-3, European Committee for Standardization, Brussels, Belgium, 2022 (Draft Version).

[6] Vanin, F., Zaganelli, D., Penna, A., Beyer, K., 2017, "Estimates for the stiffness, strength and drift capacity of stone masonry walls based on 123 quasi-static cyclic tests reported in the literature", Bull. Earthquake Engrg. 15. 10.1007/s10518-017-0188-5.

[7] Russell, A. P., and Ingham, J. M., 2010, "The influence of flanges on the in-plane seismic performance of URM walls in New Zealand buildings", Proc., NZSEE Conference, New Zealand Society of Earthquake Engrg, March 2010, Willington, New Zealand.

[8] Magenes, G., and Calvi, G. M., 1997, "In-plane seismic response of brick masonry walls", Earthquake engineering & structural dynamics 26.11: 1091-1112.

[9] Petry, S., and Beyer, K., 2014, "Influence of boundary conditions and size effect on the drift capacity of URM walls", *Engrg.Str.*, 65:76–88, doi:10.1016/j.engstruct. 2014.01.048.

[10] Pantazopoulou, S.J., 2013, "State of the Art Report for the Analysis Methods for Unreinforced Masonry Heritage Structures and Monuments", ecpfe.oasp.gr/en/node/89.

[11] Meisl, C., Elwood, K., Ventura, C., 2007, "Shake table tests on the out-of-plane response of URM walls", Canadian J. of Civil Engrg. 34. 1381-1392. 10.1139/L07-059.

[12] Doherty, K.T., 2000, “An Investigation of the Weak Links in the Seismic Load Path of Unreinforced Masonry Buildings”, Ph.D. Thesis, University of Adelaide, Australia.